Exploration of negative triangularity discharges on DIII-D

M.E. Austin[1], A. Marinoni[2], M.L. Walker[3], M.W. Brookman[1], J.S. deGrassie[3], A.W. Hyatt[3], G.R. McKee[4], C.C. Petty[3], T.L. Rhodes[5], C. Sung[5]

[1] *University of Texas-Austin, Austin (TX) USA*

[2] *Massachusetts Institute of Technology, Cambridge (MA), USA*

[3] *General Atomics, San Diego (CA), USA*

[4] *University of Wisconsin-Madison, Madison (WI), USA*

[5] *University of California-Los Angeles, Los Angeles (CA), USA*

Abstract

Discharges with negative triangularity shape were created in the DIII-D tokamak and exhibited H-mode-level confinement with L-mode-like edge behavior (no ELMs). While past experiments on DIII-D [1] demonstrated that modifications of plasma elongation can significantly change turbulence-driven transport, in this experiment a dramatic change in triangularity, from δ = +0.4 to δ = -0.4, was investigated. DIII-D's broad group of fluctuation diagnostics were employed to gain a clearer understanding of the changes in turbulence that bring about the reduced energy transport previously observed in negative triangularity discharges in the TCV tokamak [2]. The experiment also afforded the first chance to study the negative triangularity shape with neutral beam heating and $T_e \approx T_i$.

The discharges reported in this experiment were done with B_T = 2.0 T, I_p = 0.9 MA, and line averaged density of 3-4x10^{19} m^{-3}. The negative triangularity shape, shown in Fig. 1, was characterized by elongation κ = 1.4, triangularity δ = -0.4 and safety factors of q_{lim} = 4.3 or q_{95} = 3.6. The plasma was heated with up to 3.8 MW of NBI and 2.7 MW of ECH.

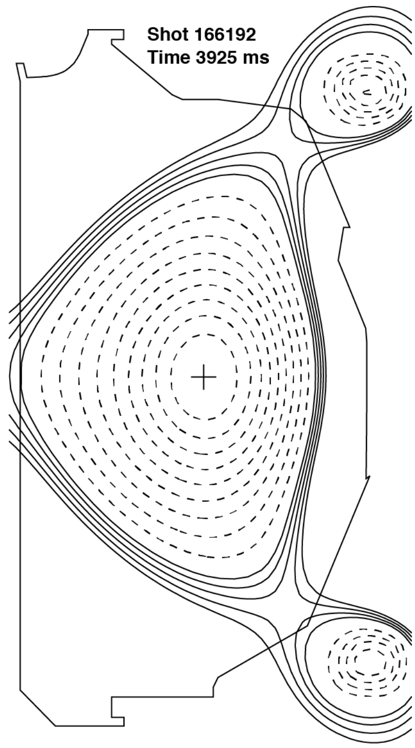

Figure 1 DIII-D EFIT reconstruction of plasma shape for negative triangularity discharge.

The time history of the discharge was divided into several phases with different heating methods, as shown in Fig. 2, to allow fluctuation data in a $T_e > T_i$ regime to be acquired during a long ECH-dominant phase followed by a shorter phase with up to three NB sources. Beam blips of 10 ms duration were used every 500 ms to obtain CER T_i and impurity rotation data. A modulated (50 Hz) ECH phase at the very beginning of the discharge flattop was used to study heat pulse propagation. Although only a limited number of discharges were made, some preliminary measurements of turbulent fluctuations were obtained.

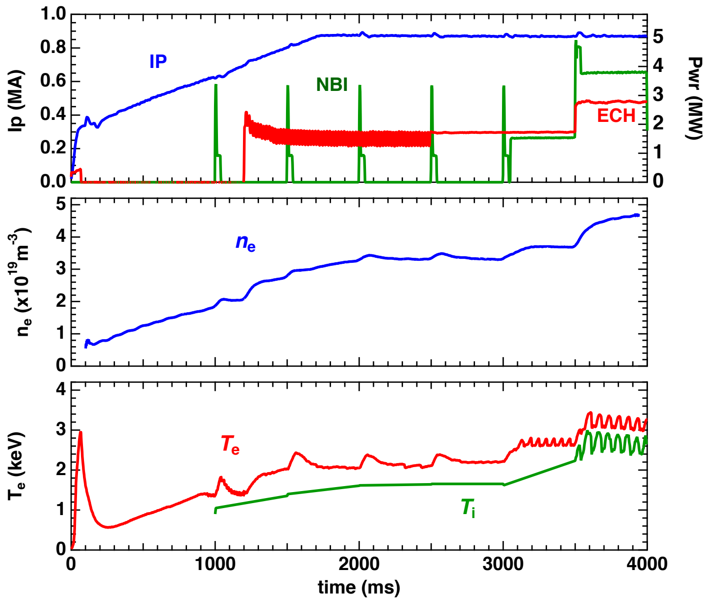

Figure 2 Time history of DIII-D negative triangularity discharge showing current and heating program, line averaged electron density and central electron and ion temperatures.

Turbulence measurements in negative triangularity discharges were made with the Correlation ECE (CECE), the Doppler Back Scattering (DBS) and the Beam Emission Spectroscopy (BES) systems. In general the fluctuation diagnostics saw reduced fluctuation levels compared with typical L-mode positive triangularity discharges from past experiments in DIII-D. An example is shown in Fig. 3 where the BES data from a discharge with δ=-0.4 is compared with a somewhat similar positive δ discharge in L-mode for a normalized radius ρ = 0.7 (where ρ is defined as the square root of toroidal flux). The negative triangularity fluctuations were approximately 20% lower than the comparison shot. It can be seen in the figure that in the δ=-0.4 case fluctuations peaked at lower frequency; the plasmas had lower rotation velocities than the positive δ case because only one NB source was used. Similar to the BES data, the DBS diagnostic saw lower fluctuation levels in negative triangularity plasmas, more like those seen in H-mode than typical L-mode discharges.

Simulations were performed with the gyro-fluid code TGLF [3] for the dominant EC heating phase of the negative triangularity discharge. Figure 4 shows histograms of growth rate and ion-electron angle of intensity versus $k_\theta \rho_s$ and minor radius. It can be seen that the growth rate is highest for $k_\theta\rho_s > 5$ and $\rho > 0.7$ while the ion-electron intensity angle is largest in the same region. This indicates that the turbulence is dominated by electron modes. Also the TGLF analysis shows that the turbulence growth rates are most sensitive to electron temperature and electron density gradient scale lengths. This electron-dominated situation is similar to what was seen in TCV [4].

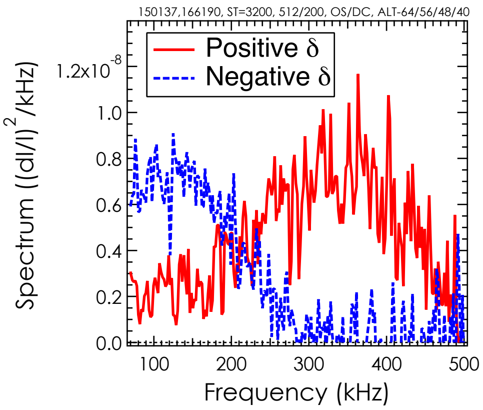

Figure 3 Electron density fluctuation spectra from the BES diagnostic for the negative triangularity experiment compared to an older positive triangularity case.

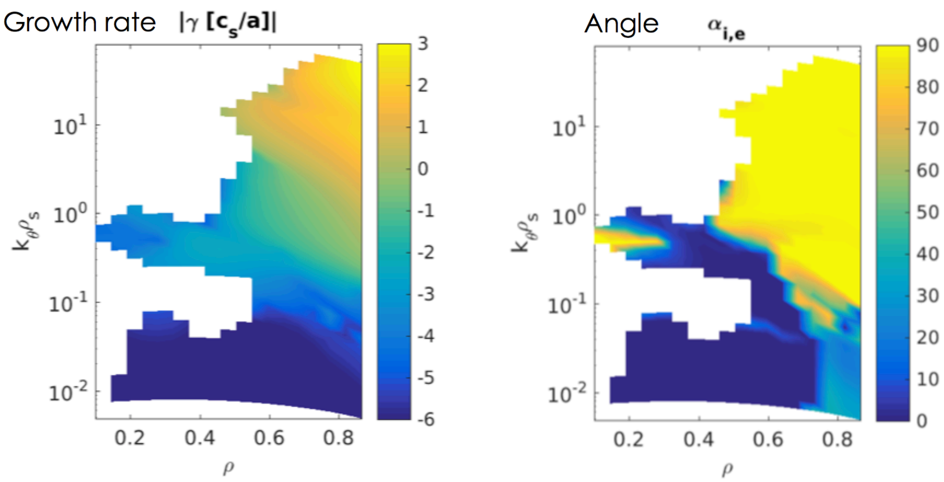

Figure 4 Histograms of growth rates and ion-electron intensity angle for a range of $k_\theta\rho_s$ and flux coordinates.

Significant signs of improved confinement were observed in the last 500 ms of these discharges, when an additional two beams were added to see how the discharge performed with dominant NB heating. ECH was kept at the same level with 2.7 MW of power. Figure 4 shows the time history of the plasma current and heating, along with the calculated normalized beta β_N and the H-mode confinement factor $H_{98,y2}$. It can be seen that β_N = 1.6

was attained with an $H_{98,y2}$ factor of 0.85, both significantly higher than typical L-mode discharges on DIII-D.

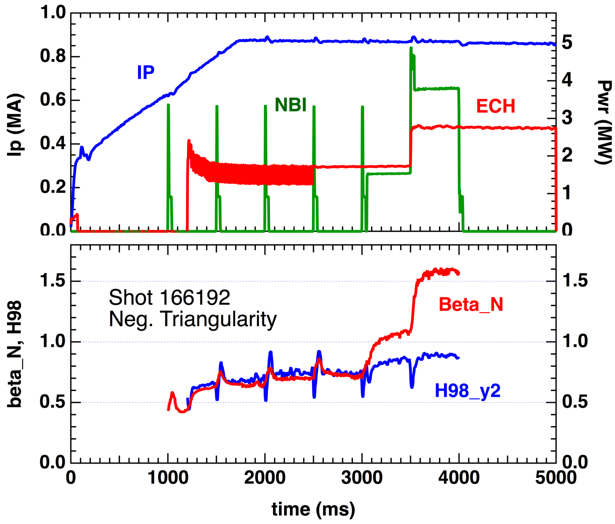

Figure 5 Time histories of heating program and confinement parameters for the DIII-D negative triangularity discharge with 3.8 MW of NBI and 2.7 MW of ECH.

Turbulence and transport in negative triangularity discharges in DIII-D have been investigated. Early results show a clear pattern of reduced fluctuation levels and improved confinement in plasmas with L-mode-like edge profiles and no ELMs. The dramatic difference in shape compared to standard “D”-shaped plasmas provides a stringent test of turbulence models. Moreover, the improved confinement, without ELMs, plus the possibility of more economically placed divertor structure makes the scenario a good prospect for future fusion reactor designs.

Acknowledgement

Work supported by the US DOE under DE-FG02-97ER54415 and DE-FC02-04ER54698. DIII-D data shown in this paper can be obtained in digital format by following the links at https://fusion.gat.com/global/D3D_DMP.

References

[1] C. Holland *et al*., Phys. Plasmas **18** (2011) 056113.

[2] Y. Camenen *et al*., Nucl. Fusion **47** (2007) 510.

[3] G. M. Staebler *et al*., Phys. Plasmas **14** (2007) 055909.

[4] A. Marinoni *et al*., Plasma Phys. Cont. Fusion **51** (2009) 055016.